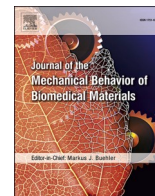




Contents lists available at ScienceDirect

Journal of the Mechanical Behavior of Biomedical Materials

journal homepage: www.elsevier.com/locate/jmbbm

Does tissue fixation change the mechanical properties of dry ovine bone extracellular matrix?

Michael Indermaur^{a,*}, Daniele Casari^b, Tatiana Kochetkova^b, Bettina M. Willie^c,
Johann Michler^b, Jakob Schwiedrzik^b, Philippe Zysset^{a,**}

^a ARTORG Center for Biomedical Engineering, University of Bern, Switzerland

^b Swiss Federal Laboratories for Material Science and Technology, Empa, Thun, Switzerland

^c Research Centre, Shriners Hospital for Children-Canada, Faculty of Dental Medicine and Oral Health Sciences, McGill University, Montreal, Canada

ABSTRACT

Tissue fixation is a prevalent method for bone conservation. Bone biopsies are typically fixed in formalin, dehydrated in ethanol, and infiltrated with polymethyl methacrylate (PMMA). Since some experiments can only be performed on fixed bone samples, it is essential to understand how fixation affects the measured material properties. The aim of this study was to quantify the influence of tissue fixation on the mechanical properties of cortical ovine bone at the extracellular matrix (ECM) level with state-of-the-art micromechanical techniques.

A small section from the middle of the diaphysis of two ovine tibias (3.5 and 5.5 years old) was cut in the middle and polished on each side, resulting in a pair of mirrored surfaces. For each pair, one specimen underwent a fixation protocol involving immersion in formalin, dehydration with ethanol, and infiltration with PMMA. The other specimen (mirrored) was air-dried. Six osteons were selected in both pairs, which could be identified in both specimens. The influence of fixation on the mechanical properties was first analyzed using micropillar compression tests and nanoindentation in dry condition. Additionally, changes in the degree of mineralization were evaluated with Raman spectroscopy in both fixed and native bone ECM. Finally, micro tensile experiments were conducted in the 3.5-year fixed ovine bone ECM and compared to reported properties of unfixed dry ovine bone ECM.

Interestingly, we found that tissue fixation does not alter the mechanical properties of ovine cortical bone ECM compared to experiments in dry state. However, animal age increases the degree of mineralization ($p = 0.0159$) and compressive yield stress ($p = 0.041$). Tissue fixation appears therefore as a valid conservation technique for investigating the mechanical properties of dehydrated bone ECM.

1. Introduction

High-resolution peripheral quantitative computed tomography (HR-pQCT) delivers accurate bone geometry and microstructure that allows individual prediction of bone strength *in vivo* using finite element analysis (FEA) (Whittier et al., 2020). However, finite element analysis requires material properties at the extracellular matrix (ECM) level as input. Those material properties have to be acquired experimentally at the ECM level, especially when a specific bone disorder needs to be investigated. The most common technique used to obtain these values is nanoindentation (Hoffler et al., 2000; Oliver and Pharr, 1992; Wolfram et al., 2010; Zysset, 2009), which measures an indentation modulus characterizing the elastic response and hardness that is related to post-elastic compaction. Recently, new methods were developed to measure the post-yield behavior of bone ECM in both compression and tension, namely, micropillar compression (Indermaur et al., 2021;

Kochetkova et al., 2020; Peruzzi et al., 2021; Schwiedrzik et al., 2014, 2017; Tertuliano and Greer, 2016) and micro tensile experiments (Casari et al., 2020, 2021).

Often, those experiments are performed in biopsies or fragments of a fracture site. However, experiments on biopsies can generally not be performed on the same day of the extraction and the tissue has to be conserved. Mostly, the biopsies are stored in a freezer at a temperature of $-20\text{ }^{\circ}\text{C}$ and thawed before the experiments. Another approach is to dehydrate the specimen in ethanol or in air. However, storage at ambient temperature without chemical fixation degrades bone tissue over time. Therefore, fixing or “chemically freezing” the biopsy with formalin is a common option. The benefit of fixation is that the tissue becomes non-hazardous. This is valuable when experiments need to be performed in laboratories that do not have the authorization to test fresh human bone tissue. A typical fixation protocol, frequently used in histology, consists of fixing the bone in a phosphate-buffered formalin

* Corresponding author.

** Corresponding author.

E-mail addresses: michael.indermaur@unibe.ch (M. Indermaur), philippe.zysset@unibe.ch (P. Zysset).

<https://doi.org/10.1016/j.jmbbm.2023.106294>

Received 22 March 2023; Received in revised form 1 July 2023; Accepted 2 December 2023

Available online 10 December 2023

1751-6161/© 2023 The Authors. Published by Elsevier Ltd. This is an open access article under the CC BY license (<http://creativecommons.org/licenses/by/4.0/>).

solution, dehydrating in ethanol, followed by a clearing with xylene, and infiltrating in polymethyl methacrylate (PMMA) (Glorieux et al., 2000).

Testing conditions have a major impact on the micromechanical properties of bone at the ECM level. Especially by comparing re-hydrated and dried non-physiological conditions. Dry bone behaves stiffer but less tough. The wet indentation modulus in the axial and transversal direction of the mineralized collagen fiber (MCF) arrays is decreased by 17% and 24% respectively (Schwiedrzik et al., 2014). The wet compressive ultimate strength in axial and transversal directions is reduced by 76% and 71% respectively (Schwiedrzik et al., 2017). Wet tensile properties were only acquired at the multilamellar level; however, the trends are similar. The ultimate tensile strength is 43 % and 69% lower in hydrated tissue for axial and transversal MCF orientation, respectively (Casari et al., 2021).

Several studies analyzed the mechanical properties of formalin or ethanol fixed bone properties at the apparent level. After 1 year of storage in formaldehyde, goat bone showed no significant difference in strength, stiffness, and energy absorption using a four-point bending test and torsion (van Haaren et al., 2008). The mechanical properties of

murine vertebrae and femurs were not significantly different between freezing and formalin fixation (elastic modulus, yield, and ultimate strength). However, the viscoelastic properties alter due to the formalin fixation (Nazarian et al., 2009). Furthermore, human and bovine bone showed no change in the elastic modulus using formalin fixation. Nevertheless, formalin fixation significantly reduces plastic energy absorption (Stefan et al., 2010). In contrast, Zhang and colleagues detected a 12% reduction in elastic modulus and a 54% increase in failure strain using formalin fixation (Zhang et al., 2016).

However, there exist only a few studies that analyzed at the micro level. Early work in 1966 has shown that hardness is increased by approximately 20% in fixed bone (24h in 10% formalin solution) compared to healthy control tissue (Weaver JK, 1966). Another study suggests that bone tissue dehydrated with ethanol and embedded in PMMA, exhibits a similar indentation modulus than dry bone tissue (Rodríguez-Florez et al., 2013). Still, hardness was found to be slightly increased (Evans et al., 1990; Rodríguez-Florez et al., 2013).

The overall goal of this study is to find a preservation technique, which allows to analyze the micromechanical properties at the ECM

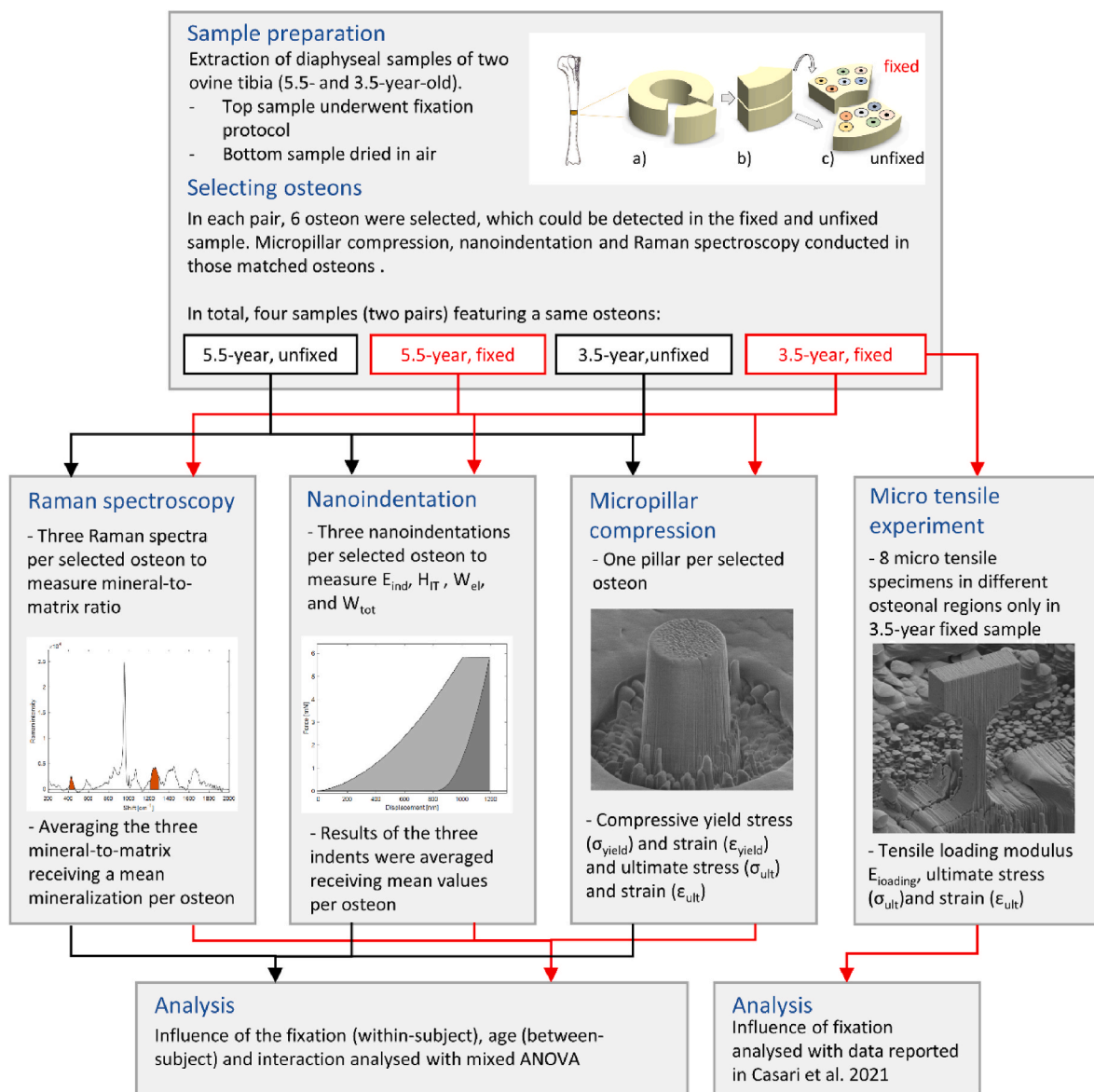


Fig. 1. Study pipeline: Sample preparation from two ovine tibias (3.5-year and 5.5-year old). The degree of mineralization was collected using Raman spectroscopy. Mechanical properties were measured on fixed and unfixed specimens using nanoindentation and micropillar compression. Additionally, micro tensile of fixed bone tissue were determined. Lastly, properties of fixed bone ECM were compared to unfixed bone ECM.

level of bone and fulfill the biosafety regulations in laboratories. Therefore, this study aims to analyze the influence of fixation with formalin, dehydration with ethanol and infiltration of PMMA on the micromechanical properties of bone ECM measured using the most recent techniques. Our working hypothesis is that the fixation procedure does not influence the mechanical properties in both compression and tension compared to dried tissue.

Micropillar compression tests are performed *in vacuo* in paired fixed and unfixed ovine bone samples, and potential differences in the mechanical outcome are analyzed. These tests are completed with nanoindentation experiments. Additionally, the degree of mineralization is assessed by Raman spectroscopy to check for a potential influence of animal age. Finally, micro tensile experiments are conducted on fixed bone ECM and compared with data from literature (see Fig. 1).

2. Materials and methods

2.1. Sample preparation

This study comprises specimens from two ovine tibias of different ages (3.5 and 5.5 years). After acquiring the tibias from a local butcher, they were stored in a freezer at -20°C until sample preparation was conducted along the following steps. First, a cortical ring (Fig. 2 a) was extracted from the middle section of the diaphysis using a diamond band saw (Exact, Norderstedt, Germany). Second, a random small section was extracted from the ring (Fig. 2 b). Lastly, this small section was cut transversely in the middle, delivering a pair of specimens with surfaces matching each other (Fig. 2 c). One specimen of the pair was dried in the air. The other specimen underwent a classical fixation protocol according to Glorieux and colleagues (Glorieux et al., 2000). The biopsy was initially fixed in a 10% phosphate-buffered formalin (pH 7.1) solution at room temperature for 72 h. Afterwards, the biopsy was dehydrated with increasing ethanol concentrations, followed by clearing with xylene. Finally, the biopsy was infiltrated in polymethylmethacrylate (PMMA) (Glorieux et al., 2000).

The four specimens (3.5y fixed, 3.5y unfixed, 5.5y fixed, and 5.5y unfixed) were glued on a scanning electron microscope (SEM) stub. Then, the specimens were lapped (Logitech PM5, Glasgow, UK) with a 1000 grit SiC powder, polished (Logitech PM5) with an ultra-fine Al_2O_3 powder (grain size $0.3\ \mu\text{m}$) and cleaned in ultra-sonic DI water bath for 60 s, providing a clean and smooth surface.

2.2. Micropillar compression

2.2.1. Micropillar fabrication

For both pairs, six osteons were selected on a light microscope image, which could be identified in both specimens (fixed and unfixed, see Fig. 2 c). Before micropillar fabrication, an 11 nm thick gold film was sputtered on the specimens (Leica EM ACE600, Wetzlar, Germany) to avoid charging during the focused ion beam (FIB) milling procedure. Micro-pillars were fabricated *in vacuo* using FIB milling following the

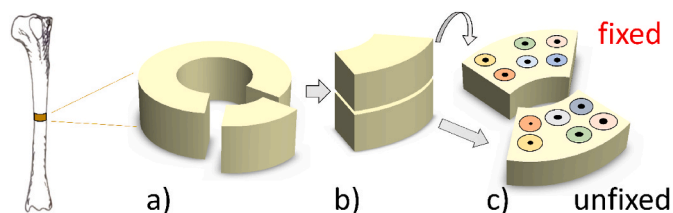


Fig. 2. Schematic overview of sample preparation. a) A cortical segment was extracted from a diaphyseal cortical ring, b) the segment was transversely cut in the middle, and c) six osteons were selected in the mirrored surfaces of the fixed and unfixed samples. As a result, the osteons were oriented along the normal of the sample surfaces.

protocol described by Indermaur and colleagues (Indermaur et al., 2021; Schwiedrzik et al., 2014) in the osteonal region (see Fig. 3). FIB-milling was done with a dual-beam instrument (Tescan Lyra, Brno, Czech Republic) consisting of a FIB and a scanning electron microscope (SEM). After FIB-milling, the micropillars revealed a final geometry of approximately $5\ \mu\text{m}$ in diameter and $10\ \mu\text{m}$ in height. The exact geometry was measured using a high-resolution scanning electron microscope (SEM, Hitachi, Tokyo, Japan). In total, 24 micropillars were produced for compression tests (3.5y-fixed $n = 6$, 3.5y-unfixed $n = 6$, 5.5y-fixed $n = 6$, and 5.5y-unfixed $n = 6$), one micropillar per osteonal region. Two micropillars failed during testing due to a calibration error of the nanoindenter. Therefore, two additional micropillars were manufactured in the same osteons as the failed micropillars to have a consistent number of micropillars within the pairs.

2.2.2. Micropillar compression test

Micropillars were quasi-statically compressed *in vacuo* using a flat-punch indenter tip mounted on a nanoindenter (Alemnis, Thun, Switzerland) inside an SEM (XL30, Philips, Amsterdam, Netherland). During testing, displacements and reaction forces were recorded. The resulting force-displacement curve was corrected by accounting for the machine compliance, the sink-in of the micropillar into the bone substrate, and the toe region (the region before complete contact of indenter and micropillar). Finally, the force-displacement curves were converted into stress-strain curves. All detailed calculations are described in Indermaur et al., (2021) (Indermaur et al., 2021). From the resulting stress-strain curves, yield stress (σ_{yield}) and strain (ϵ_{yield}), and ultimate stress (σ_{ult}) and strain (ϵ_{ult}) were extracted. The point of yielding was defined by the intersection point of the stress-strain curve and the 0.2% strain offset of the loading modulus.

2.3. Nanoindentation

After micropillar compression, the gold layer on the top surface of each specimen was removed by an additional polishing cycle of approximately $1\ \mu\text{m}$ depth (Al_2O_3 powder, grain size $0.3\ \mu\text{m}$, Logitech PM5). After polishing, the trenches of the micropillar were still visible. Around each trench of the micropillar, three nanoindentation measurements were made (see Fig. 3). Indentation measurements were performed using a nanoindentation tester (Ultra Nano Hardness Tester, CSM Instruments, Peseux, Switzerland) equipped with a Berkovich tip. A trapezoidal load control protocol was used (Schwiedrzik et al., 2014). First, the indenter was pushed into the substrate with a force rate of $100\ \text{mN}/\text{min}$, reaching a final depth of $1\ \mu\text{m}$. Then the indenter was kept at the same force for 30 s. Lastly, the indenter was unloaded with a rate of

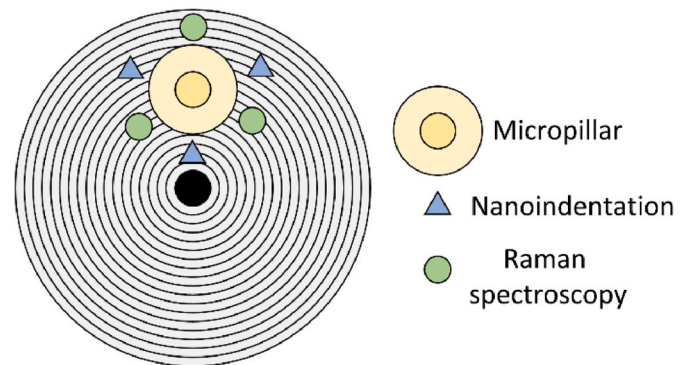


Fig. 3. Schematic overview of the conducted measurements in an osteonal region. One micropillar was fabricated in the osteonal region. Around the trench of the micropillar, three nanoindentation and Raman spectroscopy measurements were performed. The properties from the nanoindentation and Raman spectroscopy were then averaged resulting in an averaged nanoindentation and Raman spectroscopy properties per osteonal region.

400 mN/min. Indentation modulus (E_{ind}), hardness (H_{IT}), elastic (W_{el}), and total (W_{tot}) work were computed (Oliver and Pharr, 1992; Wolfram et al., 2010). Finally, the results (E_{ind} , H_{IT} , W_{el} , and W_{tot}) of the three nanoindentations around the micropillar were averaged.

2.4. Raman spectroscopy

Raman spectra were collected using a confocal upright Raman spectroscope (Ntegra-Spectra, NT-MDT, Moscow, Russia). Around each trench of the micropillar, three Raman spectra (see Fig. 3) were recorded (60 s exposure time, 633 nm wavelength, $50 \times$ objective with 0.75 numerical aperture and approximately $1.1 \mu\text{m}^3$ spot size). After background correction (Python, second-order polynomial fit for local minima, numpy. polyfit), the peaks of interest corresponding to the mineral (secondary phosphate $\nu_2\text{PO}_4$: $410\text{--}460 \text{ cm}^{-1}$) and organic (amide III: $1215\text{--}1300 \text{ cm}^{-1}$) fraction of bone were fitted (Python, non-linear least squares fit with the double-Lorentzian function, curve_fit from scipy. optimize). Consequently, the integral area of these peaks' ratio was used to estimate the mineral-to-matrix value ($\nu_2\text{PO}_4$ /amide III). Detailed spectra processing steps are described elsewhere (Kochetkova 2020 JMBBM). We chose these peaks ratio as it is polarization independent and it was shown to correlate with the calcium content in bone (Roschger et al., 2014). Finally, the three mineral-to-matrix ratios of each osteon were averaged, receiving a mean value of the osteonal degree of mineralization.

2.5. Micro tensile experiment

T-bar shaped micro tensile specimens (gauge size: $10 \times 5 \times 2 \mu\text{m}^3$) were fabricated in osteonal bone in the fixed sample of the 3.5-year-old sheep according to the protocol described by Casari and colleagues (Casari et al., 2020). Beforehand, the top surface was lapped and polished to remove the trenches of the micropillar compression tests (Logitech PM5). Osteonal bone regions had to be exposed for FIB-milling of the T-bar-shaped micro tensile specimens. Therefore, a step of approximately 0.5 mm was milled through primary osteon using a conventional milling machine. In total, 8 tensile specimens were fabricated in four exposed osteonal regions (two specimens per osteon) following the protocol of Casari and colleagues (Casari et al., 2020). The manufacturing process to produce one micro tensile experiment was approximately 6h.

The eight tensile specimens were quasi-statically loaded in tension until failure with a displacement rate of 5 nm/s (strain-rate $\approx 0.0005\text{s}^{-1}$) using a micro tensile setup (Alemnis, Thun, Switzerland) inside an SEM (*in vacuo*, Tescan Mira, Brno, Czech Republic). During testing, the force-displacement behavior was captured. Finally, force-displacement curves were converted into stress-strain curves, according to Casari et al. (2020). From the resulting stress-strain curves, the loading modulus ($E_{loading}$, highest slope in the loading curve), ultimate strain (ϵ_{ult}), and ultimate stress (σ_{ult}) were extracted, as described in Casari et al. (2020).

2.6. Statistics

The statistical analysis was performed in R (v4.1.2). The influence of age (between-subject), the condition (within-subject), and their interaction were tested with a mixed ANOVA test on the micropillar compression, nanoindentation, and Raman spectroscopy results. However, first, normal assumption (QQ plot and Shapiro test), homogeneity of variance assumption (Levene test), homogeneity of covariances assumption (Box's M-test), and extreme outliers were checked. For some variables, extreme outliers were detected. Therefore, the data were further analyzed with a robust mixed ANOVA test (R-package = WRS2) which accounts for extreme outliers. Additionally, the individual effect of fixation on the osteon was checked using a paired T-test and its effect size d according to Cohen. If the normality assumption of the difference

was not fulfilled, paired Wilcoxon signed rank test and its effect size r was used of the Rstatix package.

The fixed 3.5-year-old bone ECM tensile properties were compared with the reported tensile properties of the unfixed 3.5-year-old dry bone properties of the same sheep (but opposed leg) (Casari et al., 2021). The significant differences were checked with an unpaired two-tailed Student's T-test. The level of significance was set to 95% ($p < 0.05$).

3. Results

Raman spectroscopy, micropillar compression, nanoindentation, and micro tensile testing results were used to analyze the influence of bone tissue fixation and animal age. Tensile properties were only investigated in fixed bone ECM and compared to properties reported by Casari and colleagues for dry tissue (Casari et al., 2021). The results are summarized in Table 1.

The mineral-to-matrix ratio between the fixed and unfixed samples is not significantly different and the effect is small ($d = 0.429$). However, the older sheep's mineral-to-matrix ratio is 11–15 % higher ($p = 0.0159$).

Qualitatively, fixed samples do not behave differently in compression until reaching the point of ultimate strength (see Fig. 4). However, in the unfixed bone ECM softening occurs directly after reaching the ultimate strength. In contrast, the fixed sample behaves in an almost perfectly plastic manner (more information can be found in the supplementary material).

All the analyzed mechanical properties of the micropillar experiment were not significantly different between the two conditions. Only the ultimate strain tends to be larger in the fixed versus the unfixed sample, which is also presented by a moderate effect size ($d = 0.536$). However, yield strain ($p = 0.041$) and strength ($p = 0.041$) depended significantly on age. Furthermore, the older sheep tended to have a higher average ultimate strength ($p = 0.0531$).

The nanoindentation parameter (E_{ind} , H_{IT} , W_{el} , and W_{tot}) were not significantly different between condition, animal age, or interaction using the robust mixed ANOVA. However, the hardness (H_{IT}) tends to be higher with a moderate effect size ($d = 0.606$) using the paired T-test. For W_{el} , and W_{tot} , the differences were not normally distributed (Shapiro test). Therefore, paired Wilcoxon signed-rank test was used and revealed that the elastic work ($p = 0.0048$, effect size: large $r = 0.77$) is significantly increased for the fixed compared to the unfixed condition. Total work is not significantly different with a moderate effect size ($r = 0.362$).

No difference in the tensile mechanical behavior was qualitatively detected between the fixed and unfixed conditions when performing microtensile testing (see Fig. 5). In fact, loading modulus, ultimate stress, and strain were not significantly different between the two states (see Table 1).

4. Discussion and conclusion

The standard fixation procedure employed in this work did not influence the mechanical properties of bone ECM when compared to experiments performed on dry tissue. All analyzed mechanical variables were not significantly different between fixed and unfixed dry bone ECM according to the mixed ANOVA test. In an older study, microhardness was reported to be 20 % higher in fixed compared to unfixed bone (Weaver JK, 1966). The hardness in the current study was also, on average, 14.1% and 2.7% higher in fixed 3.5-year and 5.5-year than in unfixed with a moderate effect size. However, this increase was not significant. Additionally, the increase in hardness can be seen in the different post-failure behavior of the fixed (no softening) and unfixed (softening) micropillar samples in compression. This difference was also observed by Florez and colleagues and may be explained by the PMMA infiltration (Rodriguez-Florez et al., 2013). An indicator of this explanation is the significant increase of the elastic work of the

Table 1
Mean and standard deviation of the analyzed samples, p values of the robust mixed ANOVA test.

| Method | Parameter | 3.5y unfixed | 3.5y fixed | 5.5y unfixed | 5.5y fixed | p-value condition | p-value age | p-value interaction |
|-------------------------|-----------------------------------------|----------------------------|------------------|-----------------|-----------------|-------------------|---------------|---------------------|
| Raman | No. of observations | N = 6 | N = 6 | N = 6 | N = 6 | | | |
| | $\nu_2\text{PO}_4/\text{Amide III [-]}$ | 0.53 ± 0.01 | 0.50 ± 0.03 | 0.59 ± 0.03 | 0.59 ± 0.05 | 0.2973 | 0.0159 | 0.619 |
| Micropillar compression | No. of observations | N = 6 | N = 6 | N = 6 | N = 6 | | | |
| | σ_{ult} [GPa] | 0.85 ± 0.07 | 0.85 ± 0.01 | 0.90 ± 0.06 | 0.91 ± 0.05 | 0.6389 | 0.0531 | 0.6624 |
| | ϵ_{ult} [%] | 6.0 ± 0.6 | 6.2 ± 0.9 | 5.2 ± 0.9 | 6.5 ± 0.1 | 0.177 | 0.4132 | 0.2488 |
| | σ_{yield} [GPa] | 0.58 ± 0.05 | 0.57 ± 0.05 | 0.69 ± 0.07 | 0.64 ± 0.07 | 0.4582 | 0.0410 | 0.6087 |
| | ϵ_{yield} [%] | 2.7 ± 0.1 | 2.5 ± 0.3 | 2.8 ± 0.2 | 2.9 ± 0.2 | 0.5946 | 0.0410 | 0.1536 |
| Nano-indentation | No. of observations | N = 6 | N = 6 | N = 6 | N = 6 | | | |
| | E_{ind} [GPa] | 27.9 ± 2.98 | 28.6 ± 2.59 | 31.1 ± 1.88 | 28.6 ± 2.52 | 0.1203 | 0.1213 | 0.2977 |
| | H_{IT} [MPa] | 970 ± 170 | 1107 ± 158 | 1095 ± 68 | 1125 ± 53 | 0.3012 | 0.3241 | 0.5071 |
| | W_{el} [pJ] | 2047 ± 418 | 2519 ± 490 | 2342 ± 146 | 2490 ± 148 | 0.1716 | 0.4891 | 0.5951 |
| | W_{tot} [pJ] | 9283 ± 1406 | 10345 ± 1406 | 10327 ± 580 | 10344 ± 395 | 0.3837 | 0.3667 | 0.3639 |
| Micro tensile | No. of observations | N = 4 ^a | N = 8 | | | | | |
| | σ_{ult} [GPa] | $0.32 \pm 0.10^{\text{a}}$ | 0.34 ± 0.04 | – | – | 0.6332 | – | – |
| | ϵ_{ult} [%] | $1.9 \pm 0.4^{\text{a}}$ | 2.1 ± 0.2 | – | – | 0.2752 | – | – |
| | E_{Loading} [GPa] | $22.2 \pm 4.5^{\text{a}}$ | 22.3 ± 3.9 | – | – | 0.9694 | – | – |

^a Data from Casari et al., (2021)..

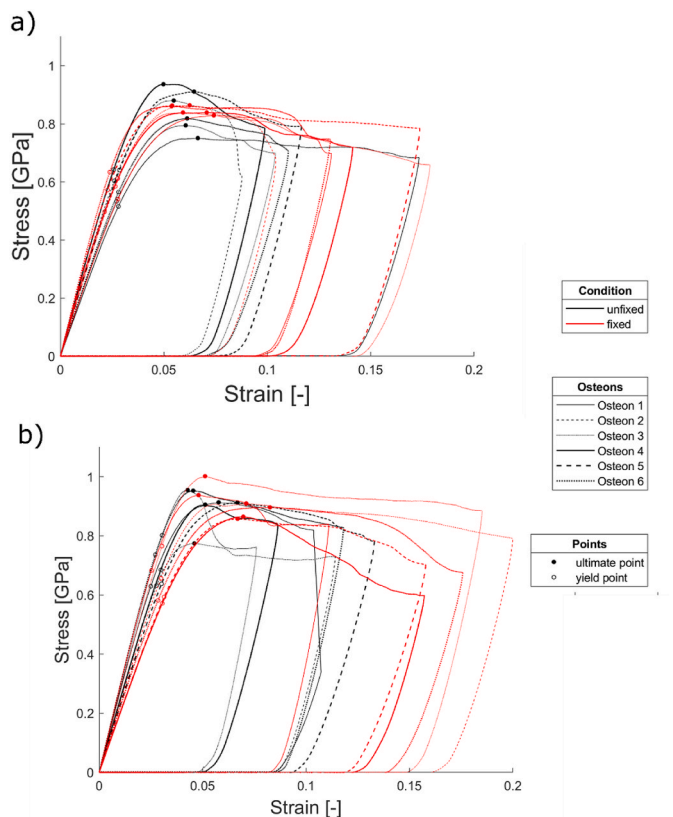


Fig. 4. Stress-strain curves of fixed (red) and unfixed (black) specimens. a) 3.5-year old sheep, and b) 5.5-year old sheep.

nanoindentation measurement, detected with the paired Wilcoxon rank sum test ($p = 0.0048$, effect size: large $r = 0.77$). As expected, no significant changes due to fixation were observed in the mineral-matrix ratio measured with Raman spectroscopy. Chemical fixation with formalin and ethanol presumably has the strongest effect on the organic components of the bone ECM, in particular the cross-links (Chapman et al., 1990; Currey et al., 1995). However, bone tissue fixation was shown to not alter the mineral density of the bone (Burkhart et al., 2010). The fact that we did not observe any differences in compressive and elastic properties of the bone ECM after fixation and embedding would support the latter statement, since these properties are largely

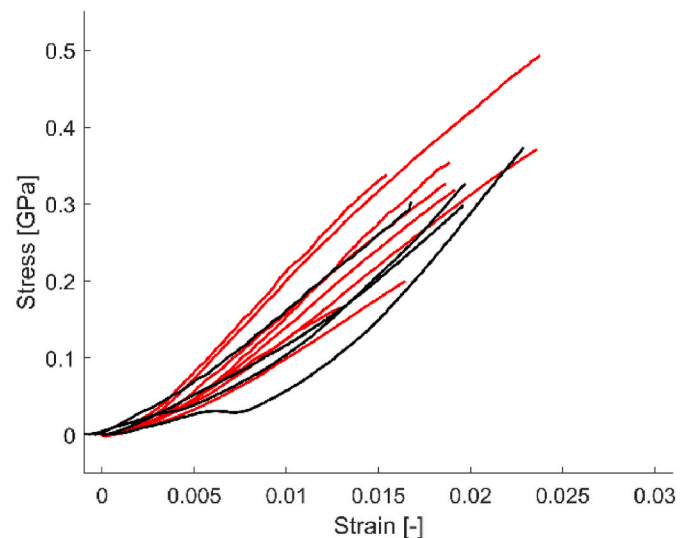


Fig. 5. Stress-strain curve of fixed (red, $n = 8$) and unfixed (black, $n = 4$) micro-tensile specimens. Unfixed samples were published in the work of Casari et al., (2021)(Casari et al., 2021).

affected by the amount and arrangement of the mineral. Additionally, we did not observe any significant differences between fixed and dried ECM in tension. The anisotropic mechanical behavior of bone ECM, proposed by Alizadeh et al., (2023), is driven by mineralized collagen fibrils, extra fibrillar matrix and their non-collagenous interface (Alizadeh et al., 2023). According to this model, axial tensile properties of bone ECM are dominated by brittle MCF rupture in dry condition as opposed to more ductile MCF pull-out observed in wet conditions. Our finding suggests that in the absence of water, the tensile strength of the MCF is not affected by fixation. In other words, fixation would not alter the interaction between collagen and intrafibrillar mineral present in dry bone.

The measured mechanical behavior and properties of the unfixed ovine tibias are in a similar range to reported values on ovine dry native tibia bone ECM. Micropillar compression in the axial direction of a 2-year old ovine tibia revealed compressive ultimate and yield strength of 0.75 ± 0.06 GPa and 0.49 ± 0.10 GPa, respectively (Schwiedrzik et al., 2014). The indentation modulus, hardness, elastic and total work in the same 2-year old tibia were 27.5 ± 2.2 GPa, 1.01 ± 0.13 GPa, 1837 ± 258 pJ, and 8069 ± 1012 pJ, respectively (Schwiedrzik et al., 2014).

The results of the unfixed 3.5-year and 5.5-year samples in the present study are in a similar range, although slightly higher. This increase can be explained by the higher degree of mineralization of older sheep. Unfortunately, Schwiedrzik and colleagues reported only the polarization-dependent mineral to matrix ratio ($v_1\text{PO}_4/\text{amideI}$), which cannot be directly compared to the polarization-independent mineral-to-matrix ratio ($v_2\text{PO}_4/\text{amideIII}$), estimated in the current work.

Age significantly increases the degree of mineralization and the point of yielding in compression in the present study. Additionally, a trend was detected that the ultimate compressive strength is higher in the 5.5-years old sheep. This agrees with the finding of Indermaur and colleagues (Indermaur et al., 2021). They showed that the mechanical properties of healthy control and three different types of Osteogenesis Imperfecta (OI) human bone ECM are increasing with the degree of mineralization.

This study is limited by its *in vacuo*/dry testing condition, which is not a physiological condition. However, the main objective of this study was to detect the influence of fixation. Rehydration of fixed and PMMA infiltrated bone ECM may lead to an unknown artifact. Therefore, the bone tissue was tested *in vacuo*/dry. Since tissue fixation does not alter the mechanical properties of dry tissue, the mechanical properties received with fixed bone ECM can be corrected with the known relationship between dry and rehydrated bone ECM (Casari et al., 2021; Schwiedrzik et al., 2017). The re-/hydrated axial indentation modulus, the axial micropillar compressive ultimate strength and axial micro tensile ultimate strength are 17%, 76%, and 43% lower compared to dry axial properties.

Another limitation of the study is the low number of samples due to the significant amount of time needed to manufacture specimens. In fact, the manufacturing time to produce the micropillars and micro tensile specimens was for both 48 machine hours (micropillars = $24 \times 2\text{h}$, and micro tensile specimens = $8 \times 6\text{h}$). Nevertheless, the study was designed to detect minimum differences in the mean of 10% (see power analysis in the supplementary materials). Regardless, an increased number of specimens may detect smaller differences.

In conclusion, the influence of tissue fixation was analyzed on dry ovine bone ECM with state-of-the-art techniques. Tissue fixation does not compromise the mechanical properties when compared to the dry state. It is, therefore, a valuable technique to preserve tissue for investigating mechanical properties of dry bone tissue at the ECM level. In addition, age significantly increases the degree of mineralization, resulting in increased yielding properties of ovine bone.

CRedit authorship contribution statement

Michael Indermaur: Conceptualization, Data curation, Formal analysis, Investigation, Methodology, Project administration, Visualization, Writing – original draft, Writing – review & editing. **Daniele Casari:** Investigation, Methodology, Writing – review & editing. **Tatiana Kochetkova:** Investigation, Methodology, Software, Writing – review & editing. **Bettina M. Willie:** Methodology, Writing – review & editing. **Johann Michler:** Resources, Writing – review & editing. **Jakob Schwiedrzik:** Conceptualization, Formal analysis, Investigation, Methodology, Resources, Writing – review & editing. **Philippe Zysset:** Writing – review & editing, Conceptualization, Formal analysis, Funding acquisition, Investigation, Methodology, Supervision, Writing – original draft.

Declaration of competing interest

All authors have no conflict of interest.

Data availability

Data will be made available on request.

Acknowledgment

We acknowledge the Swiss National Science Foundation (SNF grant #165510) and Special Focus Area Personalized Health and Related Technologies (iDoc Project 2017–304, TK) for financial support. We thank Dr. Frank Rauch and his laboratory at Shriners Hospitals for Children-Canada for performing the fixation protocol on our ovine specimens. The authors acknowledge the head of the machine shop Urs Rohrer from the ARTORG Center for Biomedical Engineering of the University of Bern for using their equipment.

Appendix A. Supplementary data

Supplementary data to this article can be found online at <https://doi.org/10.1016/j.jmbbm.2023.106294>.

References

- Alizadeh, E., Omairey, S., Zysset, P., 2023. Investigating the post-yield behavior of mineralized bone fibril arrays using a 3D non-linear finite element unit-cell model. *J. Mech. Behav. Biomed. Mater.* 139, 105660 <https://doi.org/10.1016/j.jmbbm.2023.105660>.
- Burkhardt, K.J., Nowak, T.E., Blum, J., Kuhn, S., Welker, M., Sternstein, W., Mueller, L.P., Rommens, P.M., 2010. Influence of formalin fixation on the biomechanical properties of human diaphyseal bone. *Biomed. Tech.* 55, 361–365. <https://doi.org/10.1515/BMT.2010.043>.
- Casari, D., Kochetkova, T., Michler, J., Zysset, P., Schwiedrzik, J., 2021. Microtensile failure mechanisms in lamellar bone: influence of fibrillar orientation, specimen size and hydration. *Acta Biomater.* 131, 391–402. <https://doi.org/10.1016/j.actbio.2021.06.032>.
- Casari, D., Michler, J., Zysset, P., Schwiedrzik, J., 2020. Microtensile properties and failure mechanisms of cortical bone at the lamellar level. *Acta Biomater.* <https://doi.org/10.1016/j.actbio.2020.04.030>.
- Chapman, J.A., Tzaphlidou, M., Meek, K.M., Kadler, K.E., 1990. The collagen fibril—a model system for studying the staining and fixation of a protein. *Electron. Microsc. Rev.* 3, 143–182.
- Currey, J.D., Brear, K., Zioupos, P., Reilly, G.C., 1995. Effect of formaldehyde fixation on some mechanical properties of bovine bone. *Biomaterials* 16, 1267–1271. [https://doi.org/10.1016/0142-9612\(95\)98135-2](https://doi.org/10.1016/0142-9612(95)98135-2).
- Evans, G.P., Behiri, J.C., Currey, J.D., Bonfield, W., 1990. Microhardness and Young's modulus in cortical bone exhibiting a wide range of mineral volume fractions, and in a bone analogue. *J. Mater. Sci. Mater. Med.* 1, 38–43. <https://doi.org/10.1007/BF00705352>.
- Glorieux, F.H., Travers, R., Taylor, A., Bowen, J.R., Rauch, F., Norman, M., Parfitt, A.M., 2000. Normative data for iliac bone histomorphometry in growing children. *Bone* 26, 103–109. [https://doi.org/10.1016/S8756-3282\(99\)00257-4](https://doi.org/10.1016/S8756-3282(99)00257-4).
- Hoffler, C.E., Moore, K.E., Kozloff, K., Zysset, P.K., Brown, M.B., Goldstein, S.A., 2000. Heterogeneity of bone lamellar-level elastic moduli. *Bone* 26, 603–609. [https://doi.org/10.1016/S8756-3282\(00\)00268-4](https://doi.org/10.1016/S8756-3282(00)00268-4).
- Indermaur, M., Casari, D., Kochetkova, T., Peruzzi, C., Zimmermann, E., Rauch, F., Willie, B., Michler, J., Schwiedrzik, J., Zysset, P., 2021. Compressive strength of iliac bone ECM is not reduced in Osteogenesis Imperfecta and increases with mineralization. *J. Bone Miner. Res.* 36, 1364–1375. <https://doi.org/10.1002/jbmr.4286>.
- Kochetkova, T., Peruzzi, C., Braun, O., Overbeck, J., Maurya, A.K., Neels, A., Calame, M., Michler, J., Zysset, P., Schwiedrzik, J., 2020. Combining polarized Raman spectroscopy and micropillar compression to study microscale structure-property relationships in mineralized tissues. *Acta Biomater.* 119, 390–404. <https://doi.org/10.1016/j.actbio.2020.10.034>.
- Nazarian, A., Hermansson, B.J., Muller, J., Zurakowski, D., Snyder, B.D., 2009. Effects of tissue preservation on murine bone mechanical properties. *J. Biomech.* 42, 82–86. <https://doi.org/10.1016/j.jbiomech.2008.09.037>.
- Oliver, W.C., Pharr, G.M., 1992. An improved technique for determining hardness and elastic modulus using load and displacement sensing indentation experiments. *J. Mater. Res.* 7.
- Peruzzi, C., Ramachandramoorthy, R., Groetsch, A., Casari, D., Grönquist, P., Rüggeberg, M., Michler, J., Schwiedrzik, J., 2021. Microscale compressive behavior of hydrated lamellar bone at high strain rates. *Acta Biomater.* 131, 403–414. <https://doi.org/10.1016/j.actbio.2021.07.005>.
- Rodriguez-Florez, N., Oyen, M.L., Shefelbine, S.J., 2013. Insight into differences in nanoindentation properties of bone. *J. Mech. Behav. Biomed. Mater.* 18, 90–99. <https://doi.org/10.1016/j.jmbbm.2012.11.005>.
- Roschger, A., Gamsjaeger, S., Hofstetter, B., Masic, A., Blouin, S., Messmer, P., Berzlanovich, A., Paschalis, E.P., Roschger, P., Klaushofer, K., Fratzl, P., 2014. Relationship between the $v_2\text{PO}_4/\text{amide III}$ ratio assessed by Raman spectroscopy and the calcium content measured by quantitative backscattered electron microscopy in healthy human osteonal bone. *J. Biomed. Opt.* 19, 065002 <https://doi.org/10.1117/1.jbo.19.6.065002>.
- Schwiedrzik, J., Raghavan, R., Bürki, A., Lenader, V., Wolfram, U., Michler, J., Zysset, P., 2014. In situ micropillar compression reveals superior strength and ductility but an

- absence of damage in lamellar bone. *Nat. Mater.* 13, 740–747. <https://doi.org/10.1038/nmat3959>.
- Schwiedrzik, J., Taylor, A., Casari, D., Wolfram, U., Zysset, P., Michler, J., 2017. Nanoscale deformation mechanisms and yield properties of hydrated bone extracellular matrix. *Acta Biomater.* 60, 302–314. <https://doi.org/10.1016/j.actbio.2017.07.030>.
- Stefan, U., Michael, B., Werner, S., 2010. Effects of three different preservation methods on the mechanical properties of human and bovine cortical bone. *Bone* 47, 1048–1053. <https://doi.org/10.1016/j.bone.2010.08.012>.
- Tertuliano, O.A., Greer, J.R., 2016. The nanocomposite nature of bone drives its strength and damage resistance. *Nat. Mater.* 15, 1195–1202. <https://doi.org/10.1038/nmat4719>.
- van Haaren, E.H., van der Zwaard, B.C., van der Veen, A.J., Heyligers, I.C., Wuisman, P.I. J.M., Smit, T.H., 2008. Effect of long-term preservation on the mechanical properties of cortical bone in goats. *Acta Orthop.* 79, 708–716. <https://doi.org/10.1080/17453670810016759>.
- Weaver, J.K., 1966. The microscopic hardness of bone. *J Bone Jt Surg* 48, 273–288.
- Whittier, D.E., Boyd, S.K., Burghardt, A.J., Paccou, J., Ghasem-Zadeh, A., Chapurlat, R., Engelke, K., Bouxsein, M.L., 2020. Guidelines for the assessment of bone density and microarchitecture in vivo using high-resolution peripheral quantitative computed tomography. *Osteoporos. Int.* 31, 1607–1627. <https://doi.org/10.1007/s00198-020-05438-5>.
- Wolfram, U., Wilke, H.J., Zysset, P.K., 2010. Rehydration of vertebral trabecular bone: influences on its anisotropy, its stiffness and the indentation work with a view to age, gender and vertebral level. *Bone* 46, 348–354. <https://doi.org/10.1016/j.bone.2009.09.035>.
- Zhang, G.-J., Yang, J., Guan, F.-J., Chen, D., Li, N., Cao, L., Mao, H., 2016. Quantifying the effects of formalin fixation on the mechanical properties of cortical bone using beam theory and optimization methodology with specimen-specific finite element models. *J. Biomech. Eng.* 138 <https://doi.org/10.1115/1.4034254>.
- Zysset, P.K., 2009. Indentation of bone tissue: a short review. *Osteoporos. Int.* 20, 1049–1055. <https://doi.org/10.1007/s00198-009-0854-9>.